Chapter 1

Higgs Production Through Gluon Fusion

Gluon fusion is one of the most promising production channels for Higgs bosons at the LHC, and therefore the calculations of production cross sections for this process have been of great interest. As discussed in Chapter 1, in the Standard Model gluon fusion is the dominant channel to produce a pair of Higgs bosons through a quark loop of triangle and box. Even beyond the SM, in the MSSM, gluon fusion is the major source of neutral Higgs bosons at the LHC for lower values of $tan\beta$. This chapter presents a study of the production of neutral Higgs bosons with a gluon pair via quark loop followed by (a) Higgs decays into two pairs of bottom quarks ($gg \to \phi^0\phi^0 + X \to b\bar{b}b\bar{b} + X$) and (b) One Higgs decays into a $b\bar{b}$ pair and the other Higgs decays into leptons ($gg \to \phi^0\phi^0 + X \to b\bar{b}\tau^+\tau^- + X \to b\bar{b}lj_\tau + \not{E}_T + X$). These processes were studied in the SM for the Higgs that has already been discovered with a mass 125.0 GeV and in the MSSM for the three neutral Higgses h^0, H^0 or A^0 in the mass region of $100 - 1000$ GeV.

1.1 Two Higgs Production

Fig. 1.1 represents the diagrams contributing to pair production of SM Higgs bosons via the gluon fusion process $gg \to hh$. As can be seen from the Fig. 1.1, gluon fusion has contributions from the virtual box diagram and the virtual triangle diagram. In the triangle diagram, an off shell Higgs is produced and decays into two real Higgses via the three Higgs self couplings.

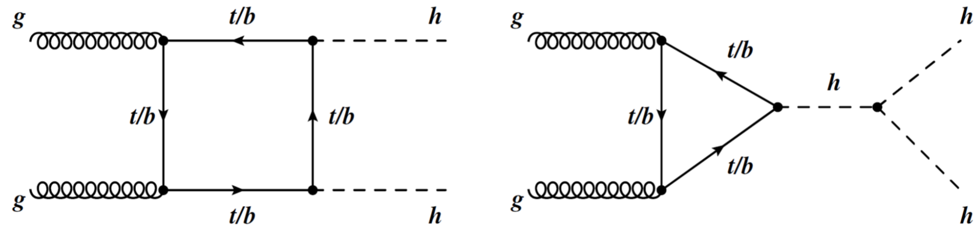

Figure 1.1: Generic diagrams contributing to pair production of SM Higgs bosons in gluon-gluon collisions (left) via box diagram and (right) via triangle diagrams.

1.2 Calculation tools for the signal

The cross section of two Higgs production at LHC via gluon fusion was evaluated with center of mass energy $\sqrt{s} = 14$ TeV. This process includes box and triangle diagrams given in Fig. 1.1 on the order of α_s^2. Along the box and triangle loops, the intermediate fermions are massive third generation quarks. The Yukawa couplings given in Appendix B were calculated using quark masses of $m_t = 173.1$ GeV and $m_b = 4.7$ GeV. For the calculation of strong coupling, the renormalization scale is set to be $\mu_R = \sqrt{\hat{s}}$, which is the parton center of mass energy. The signal cross sections were computed using MSTW2008 [1] parton distribution functions(pdfs) with the factorization scale $\mu_F = \sqrt{\hat{s}}$. The transition amplitudes for loops were calculated using a tensor reduction procedure explained by Passarino and Veltmann [2]. All tensors were reduced to scalar integrals in terms of D_0, C_0, B_0 and A_0 using FORM [3]. Two Higgs signals were generated using a Monte Carlo program with the amplitudes calculated by FORM. In order to include the higher order corrections, the results were multiplied by a K factor. K factors for $E_{CM} = 14$ TeV were calculated using the formulas given in [4],

$$\frac{\sigma_{NNLO}}{\sigma_{NLO}} = 1.149 - 0.326 \left(\frac{E_{CM}}{1\ TeV}\right)^{-1} + 0.327 \left(\frac{E_{CM}}{1\ TeV}\right)^{-\frac{1}{2}} \tag{1.1}$$

$$\frac{\sigma_{NNLO}}{\sigma_{LO}} = 1.242 - 7.17 \left(\frac{E_{CM}}{1\ TeV}\right)^{-1} + 5.77 \left(\frac{E_{CM}}{1\ TeV}\right)^{-\frac{1}{2}} \tag{1.2}$$

The above discussed tools were used throughout this chapter unless otherwise specifically mentioned in each section.

1.3 Numerical Results

1.3.1 Standard Model Higgs : $gg \longrightarrow hh$

In Fig. 1.1, h is SM Higgs with mass 125.5 GeV. The production cross section is calculated for SM Higgs, and the individual contributions from triangle diagram and box diagrams and the total cross sections are presented in Table 1.1. The results were also compared with the cross sections presented in Florian et.al [4] and found to agree within the uncertainty. As we can see from the results, the contribution from box diagrams are much larger than the total because the triangle and box diagrams interfere destructively. The next to the leading order(NLO) cross section for the production of SM Higgs pairs via gluon fusion was calculated with a K factor of 1.88 for $\sqrt{s} = 14$ TeV, and the results were compared to the cross sections presented in recent studies. See Table 1.2 for numerical values.

Contribution	$M_h = 125.5$ GeV
TRIANGLE	5.16
BOX	37.8
TOTAL	17.9

Table 1.1: Leading order cross section in fb for Standard Model Higgs pair production via gluon fusion for the LHC running at 14 TeV.

Reference	$\sigma_{NLO}^{gg\to hh}$ fb
Florian et.al[4]	33.2
Baglio et.al [5]	33.89
This study	33.6

Table 1.2: Next to the leading order(NLO) cross section in fb for Standard Model Higgs pair production via gluon fusion at the LHC for 14 TeV.

1.3.2 Higgs decay into $b\bar{b}$

Each Higgs produced here decays into $b\bar{b}$. The cross section for $pp \to (h \to b\bar{b})(h \to b\bar{b})$ was calculated using the Narrow Width Approximation (NWA) so that

$$\sigma(pp \to \phi^0\phi^0 \to b\bar{b}b\bar{b} + X) = \sigma(pp \to \phi^0\phi^0 + X) \times B(\phi^0 \to b\bar{b}) \times B(\phi^0 \to b\bar{b}) \quad (1.3)$$

where $B(\phi^0 \to b\bar{b})$ is the branching fraction of the Higgs boson decaying into $b\bar{b}$. We also applied the basic acceptance cuts for the final states at LHC with integrated luminosity $L = 30\ fb^{-1}$ and $\sqrt{s}\ =\ 14$ TeV. High Transverse momentum (P_T) trigger is required by LHC detectors for the final state b quarks. Here we apply $P_T(b) > 25\, GeV$ for the transverse momentum of final state b quarks. Fig. 1.2 represents the transverse-momentum distribution of the final state bottom quarks ($b\, or\, \bar{b}$) and as can be seen in the Fig. 1.2, the bottom quarks are ordered according to their transverse momenta, $p_T(b_1) \geq P_T(b_2) \geq P_T(b_3) \geq P_T(b_4)$.

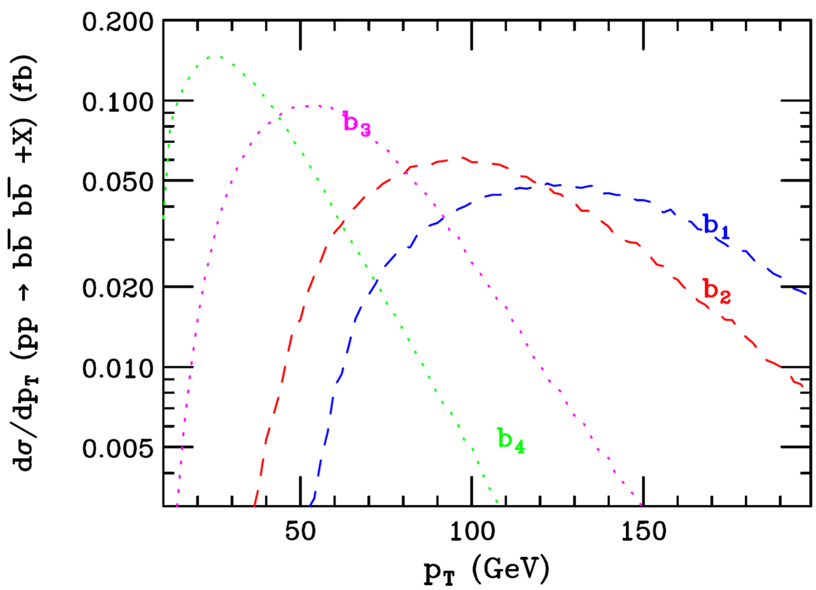

Figure 1.2: The transverse momentum distribution for the final b quarks produced, generating the SM Higgs signal from $pp \to hh \to b\bar{b}b\bar{b}$.

The pseudorapidity(η) for light particles can be defined as,

$$\eta = -ln\left[tan\left(\frac{\theta}{2}\right)\right]$$

where, θ is the angle between the outgoing particle and the beam axis. For final state b quark here, we chose $|\eta_b| < 2.5$.

We also introduce a special mass cut here to save the signal from high QCD backgrounds. b_1 is the final state b which has the highest transverse momentum, and the next three jets were re ordered so that the second jet minimizes, $\Delta M_{1j} = |M_{1j} - M_\phi|$ where $j = 2, 3, 4$. According to this, two selected pairs(12 and 34) of the final state b should require $|M_{b\bar{b}} - M_\phi| \leq \Delta M_{bb}$ where $\Delta M_{bb} = 0.15 M_\phi$. Fig. 1.3 shows the invariant-mass($M_{ij}, i, j = 1, 2, 3, 4$) distribution of the final state $b_i b_j$ pairs for the Higgs signal $pp \to b\bar{b}\, b\bar{b} + X$ via $gg \to hh$ after reordering jets.

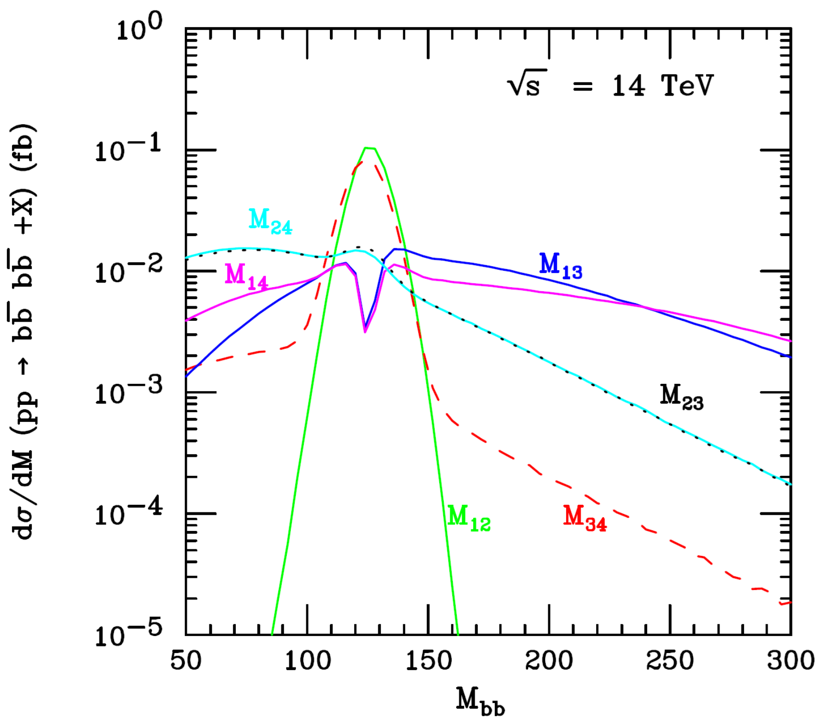

Figure 1.3: The invariant mass distribution for the Higgs signal from $gg \to hh \to b\bar{b}\, b\bar{b} + X$ with $M_h = 125.5$ GeV.

For the angle between the final state particles, we used, $\Delta R > 0.4$, where ΔR is defined by,

$$\Delta R = \sqrt{(\Delta\Phi)^2 + (\Delta\eta)^2} \tag{1.4}$$

where Φ is the angle between two particles in the transverse plane. Finally the

Gaussian smearing given below (in GeV) was applied to the outgoing momentum to approximate the detector effects.

$$\frac{\Delta E}{E} = \frac{0.5}{\sqrt{E}} \oplus 0.03 \tag{1.5}$$

Table 1.3 presents the calculated cross section for the signal $pp \to b\bar{b}b\bar{b}$ via $gg \to hh$ for the SM Higgs of mass 125.5 GeV. Appropriate branching ratio is also given in the table.

Cross section in fb	$M_h = 125.5$ GeV
$\sigma(gg \to hh \to 4b)$	3.40
BF_{bb}	0.626

Table 1.3: LO cross section in fb for $gg \to hh \to b\bar{b}b\bar{b} + X$ for the Standard Model using pdfs from MSTW2008. BFBB is the branching ratio of Higgs decaying into $b\bar{b}$.

1.3.3 Higgs decay into $\tau^+ \tau^-$

In the Standard Model, the Higgs dominantly decays into $b\bar{b}$ with branching ratio $\approx 60\%$, into WW^* with branching ratio $\approx 22\%$ and into $\tau^+\tau^-$ with branching ratio $\approx 6\%$. In this study we also considered the production of a Higgs pair via gluon fusion followed by one Higgs decaying into $b\bar{b}$ while the other decays into a pair of τ, τ^+ and τ^- which decays into lighter leptons($e^{\pm}$ or $\mu^{\pm}$), mesons($\pi/a_1/\rho$) and missing energy. The mass of the Higgs boson is much heavier than the mass of the tau leptons, and therefore the two leptons are very energetic. Hence, for the decay of tau here we use the Collinear Approximation which assumes the final particles from tau decay are almost along the same direction as its parent particles. Except for the basic cuts applied for final state $b\bar{b}$ which is explained in the previous section, we use,

$$\begin{array}{lll} P_T(j) > 15\,GeV, & P_T(l) > 20\,GeV, & P_T(j_\tau) > 40GeV \\ |\eta(j)| < 2.5, & |\eta(l)| < 2.5, & |\eta(j_\tau)| < 2.5 \\ \Delta R(jj_\tau) > 0.4, & \Delta R(lj_\tau) > 0.4, & \Delta R(lj) > 0.4 \\ \not{E}_T > 40\;GeV, & m(l,\not{E}_T) < 30\;GeV, & \phi(l,j_\tau) < 170^0 \end{array} \tag{1.6}$$

$\not{E}_T$ is the missing transverse energy, and $\phi(l, j_\tau)$ is the transverse angle between lepton and tau jet. The quantity $m(l,\not{E}_T)$ is the transverse mass of lepton and neutrino as defined in "*Collider Physics*"[6]. Gaussian smearing in GeV, for charged leptons used here can be given by,

$$\frac{\Delta\,E}{E} = \frac{0.25}{\sqrt{E}} \oplus 0.01. \tag{1.7}$$

Table 1.4 gives the calculated LO cross sections for the process $gg \to hh \to b\bar{b}\tau^+\tau^-$ followed by $\tau^+\tau^- \to lj_\tau + \not{E}_T$.

Cross section in fb	$M_h = 125.5$ GeV
$\sigma(pp \to hh \to bb\tau^+\tau^- \to b\bar{b}lj_\tau + \not{E}_T)$	0.0613

Table 1.4: LO cross section in fb for $gg \to hh \to b\bar{b}\tau^+\tau^- \to b\bar{b}lj_\tau + \not{E}_T + X$ for the Standard Model using pdfs from MSTW2008.

1.4 Production of MSSM Higgs

The mechanisms for the production of two MSSM Higgs bosons are similar to the SM, and the possible diagrams are given in Fig. 1.4. Though several combinations of neutral Higgs pairs of the MSSM can be produced through gluon fusion, here we consider the processes $pp \to h^0h^0/H^0H^0/A^0A^0$ where h^0 and H^0 are CP even light and heavy Higgs bosons in the MSSM respectively, and A^0 is CP odd pseudo scalar. The intermediate virtual Higgs boson in the triangle diagram should be either h^0 or H^0 to preserve the CP conservation at the three Higgs vertex.

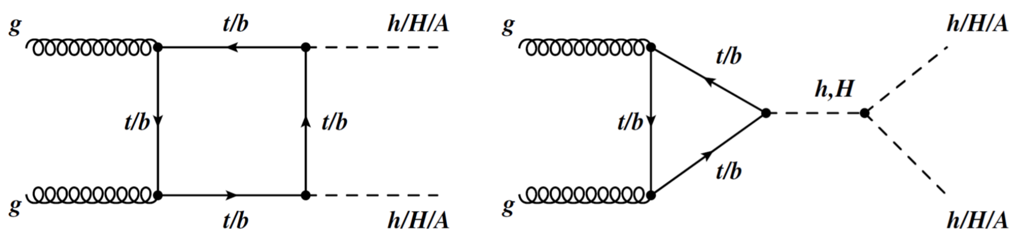

Figure 1.4: Generic diagrams contributing to pair production of MSSM Higgs bosons in gluon-gluon collisions (left) via box diagram and (right) via triangle diagrams.

1.4.1 MSSM pseudo scalar

Here we consider the production of CP even pseudo scalars via gluon fusion. The loop diagrams were evaluated using the tensor reduction explained in Passarino Veltman [2] for the Standard Model. We require several couplings including the trilinear Higgs self couplings [Appendix B] which depends on β and the mixing angle α. MSSM pseudo scalar production $gg \to A^0A^0$ was considered first and then the pseudo scalar decaying into a $b\bar{b}$ pair was evaluated. Fig 1.5 presents the calculated cross sections for $gg \to A^0A^0 + X$ for three selected $tan\ \beta$ values.

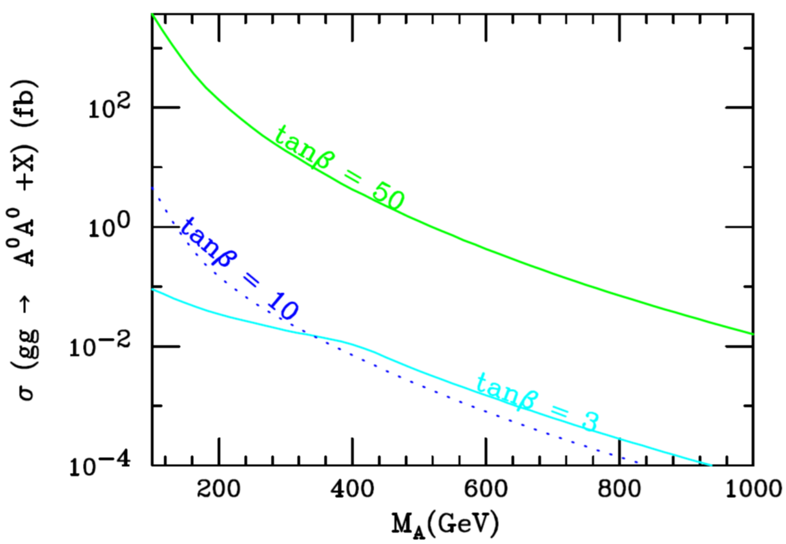

Figure 1.5: Leading order cross section for the production of pseudo scalars via gluon fusion for three different $tan\ \beta$ values.

We first consider both pseudo scalars decaying into two pairs of b so that cross sections were calculated for the process $gg \to A^0A^0 \to b\bar{b}b\bar{b} + X$. Fig. 1.6 shows the resulting cross section values after the pseudo scalar Higgs decay into b pairs, and the values are calculated for $\sqrt{s} = 14\ TeV$ and integrated luminosity $\mathcal{L} = 30\ fb^{-1}$. The same cuts, scales and pdfs were used here as explained for the Standard Model.

Next we considered the production of the MSSM pseudo scalar via gluon fusion with one Higgs decaying into a pair of b quarks and the other Higgs decaying into tau leptons followed by tau leptons with one tau decaying leptonically and the other hadronically.

The LO cross sections calculated for $pp \to\ (A^0 \to b\bar{b})(A^0 \to \tau^+\tau^- \to lj_\tau + \not{E}_T)$

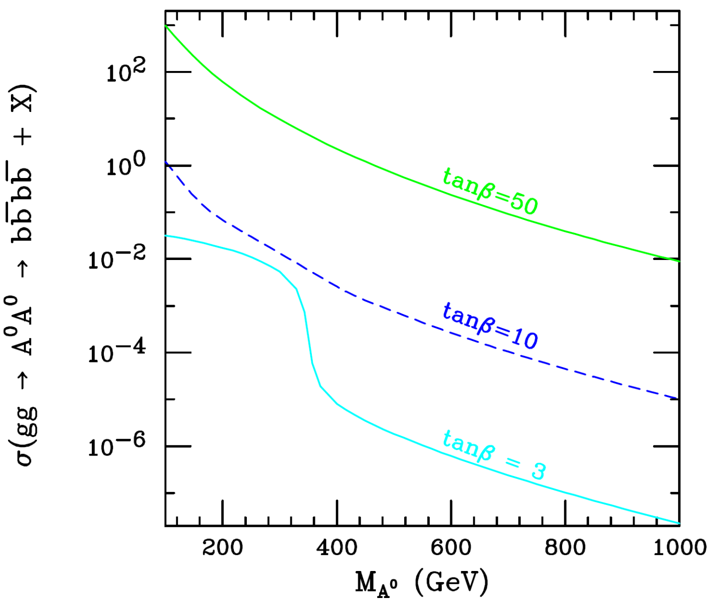

Figure 1.6: Leading Order cross section in (fb) for the process $gg \to A^0A^0 \to b\bar{b}b\bar{b} + X$.

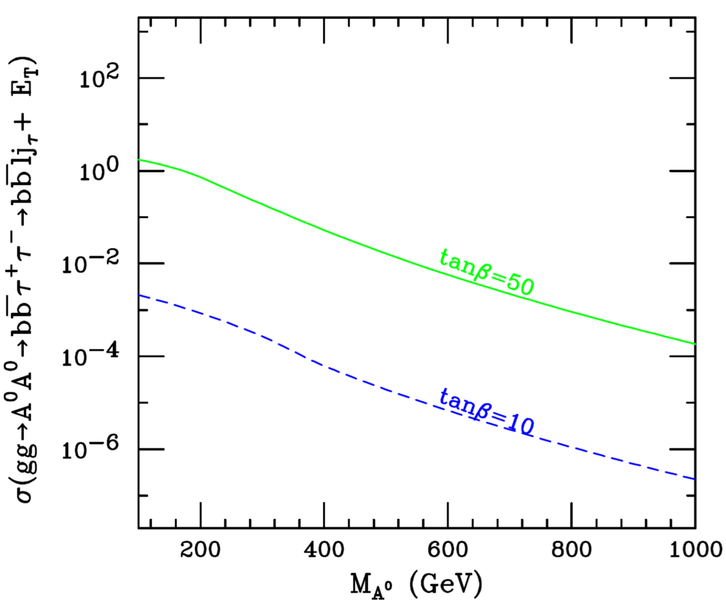

Figure 1.7: LO cross sections for the process $gg \to$ $(A^0 \to b\bar{b})(A^0 \to \tau^+\tau^- \to lj\tau + \not{E}_T$ for two different $tan\ \beta$ values.

are presented in Fig. 1.7. Except the points discussed here, all other parameters, scales, cuts and methods are the same as explained in previous sections.

1.4.2 MSSM Light Higgs

CP even light Higgs in the MSSM is considered to be almost identical to the Standard Model Higgs boson. Since the SM Higgs mass is a known parameter now, the parameter space for light Higgs can be limited to certain values. FeynHiggs 2.9.1[7] was used here in terms of calculating the light Higgs masses and related parameters. Fig.1.8 shows the light Higgs mass in the parameter space of $tan\beta$ and M_A. The three curves drawn in the Fig. 1.8 which are for $M_h = 125.5$ GeV which is the exact SM Higgs mass and other two for 122.5 GeV and 128.5 GeV. FeynHiggs requires a few variables to be inputed in text file "var.in", and this program calculates the masses of MSSM Higgs bosons and other important observables such as mixing angles, branching ratios, couplings and many more. Two sets of input parameters were considered in this case, and the light Higgs masses and related parameters were calculated accordingly. Two cases we considered here were case (a) $Msusy = 1000\ GeV$, $X_t = 2000$ GeV and case (b) $Msusy = 2000$ GeV , $X_t = (\sqrt{6} * Msusy)$. The details of all parameters of the input text file for the FeynHiggs executable is given in the Appendix C. M_A (mass of pseudo scalar) and TB($tan\beta$) which are the free parameters of the MSSM were changed over the selected ranges of values. As can be seen from two plots for $M_A > 250$ GeV, $tan\ \beta$ remains almost at a constant value in the range between 3 to 14. So we limited our calculation for selected values of $tan\ \beta$. FeynHiggs uses input variables to calculate the masses, mixing angles, branching ratios, couplings, etc. for the MSSM Higgs bosons.

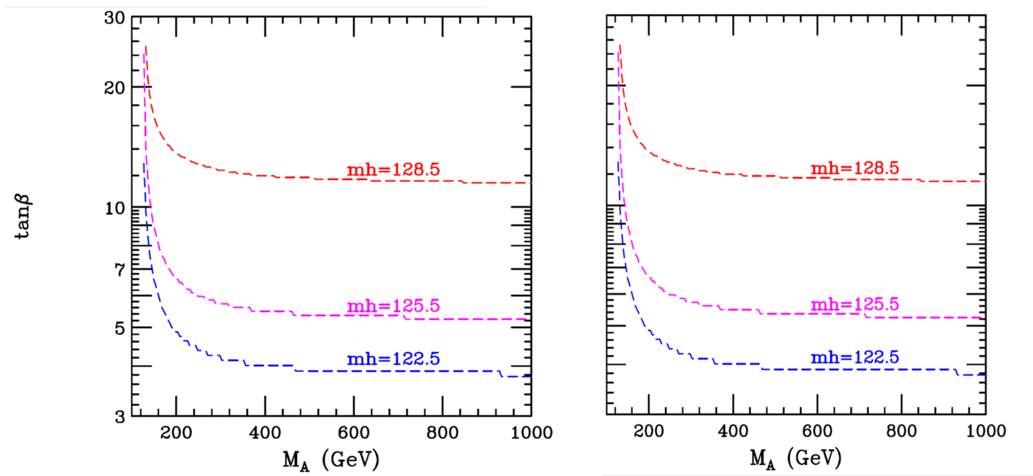

Figure 1.8: Change in light Higgs mass in the parameter space of $tan\ \beta$ vs MA. Left figure is for case(a) and right figure is for case(b) explained in the text.

The decay of Light Higgs to two pairs of $b\bar{b}$ was considered, and the cross section was calculated for the process $pp \rightarrow h^0h^0 \rightarrow b\bar{b}b\bar{b} + X$. Figure 1.9 shows the calculated cross sections(in fb) for the process for MA changing from 250 GeV to 1000GeV and for three most appropriate $tan\ \beta$ values. Pdfs and cuts used here were the same as we explained in previous sections. The two plots given in the Fig. 1.9 explain the two cases explained above according to the variables input to the FeynHiggs to produce light Higgs mass and other related parameters.

For the second step, a process where one light Higgs decay into $b\bar{b}$, and the other decays into $\tau^+\tau^-$ with the τ further decaying was considered. Cross sections calculated for this process $gg \rightarrow\ (h^0 \rightarrow b\bar{b})(h^0 \rightarrow \tau^+\tau^- \rightarrow lj_\tau + \not{E}_T)$ are graphed as a function

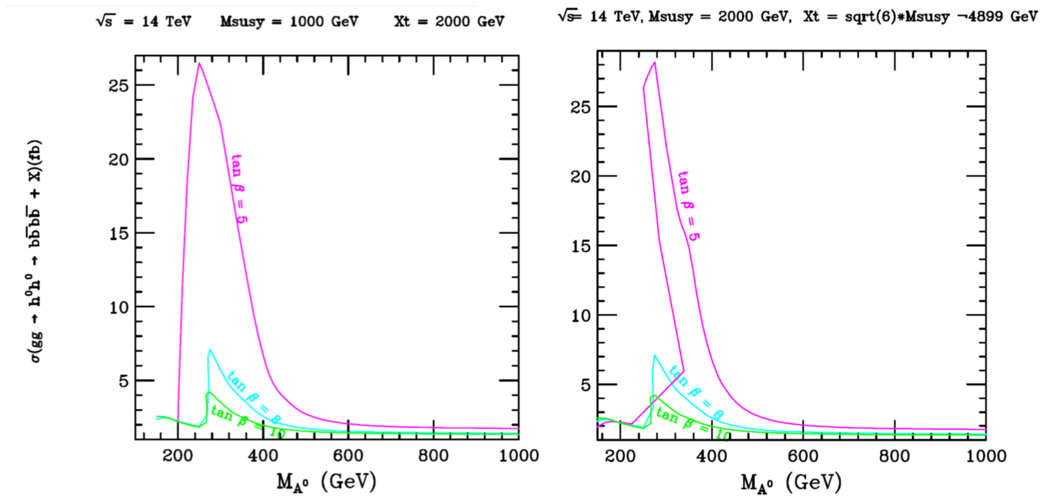

Figure 1.9: Leading order cross sections for the process $gg \to h^0h^0 \to b\bar{b}b\bar{b}+X$, where h^0 is light Higgs. Left figure is for the light Higgs generated for $M_{susy} = 1000\ GeV$, $X_t = 2000\ Gev$ and right figure is for the light Higgs generated for $M_{susy} = 2000\ GeV$, $X_t = (\sqrt{6} * M_{susy})$.

of M_A in Fig. 1.10.

1.4.3 MSSM Heavy Higgs

Fig. 1.11 shows the mass of the heavy Higgs(M_{H^0}) vs M_A and is drawn for several $tan\ \beta$ values. As can be seen from the figure for $M_A \geq\ 200$ GeV and higher $tan\ \beta$ values, the heavy Higgs is almost degenerate with the behavior of the pseudo scalar. Even with the difference of couplings heavy Higgs should reproduce the cross sections calculated for pseudo scalar.

This chapter covered the production cross sections of the signal using the mentioned processes. A detailed analysis of these values along with the backgrounds associated with them, will be discussed in Chapter 4 with the significant improvements for the

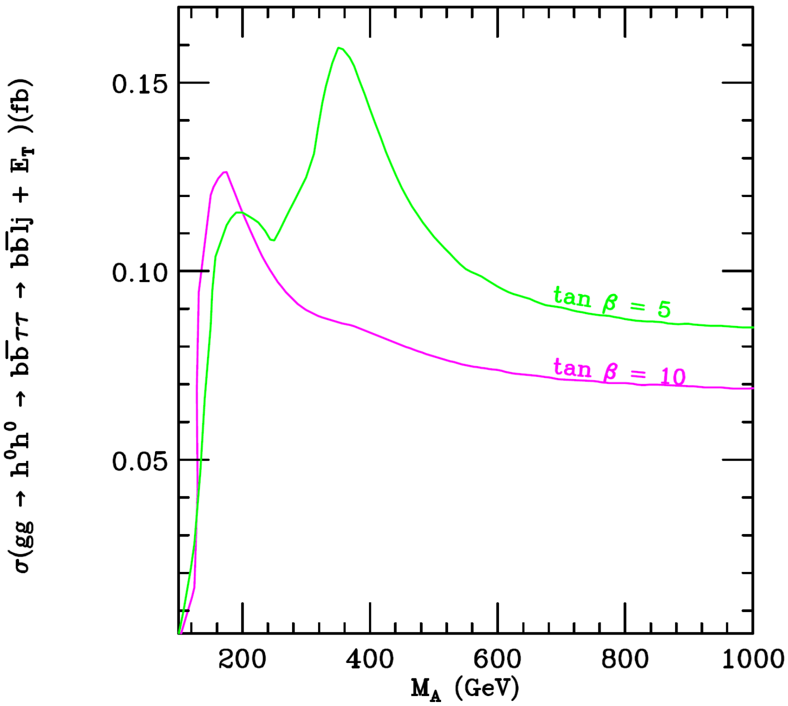

Figure 1.10: Leading order cross sections for the process $gg \to (h^0 \to b\bar{b})(h^0 \to \tau^+\tau^- \to lj_\tau + \not{E}_T)$ for $M_{susy} = 1000 GeV$.

4b final state.

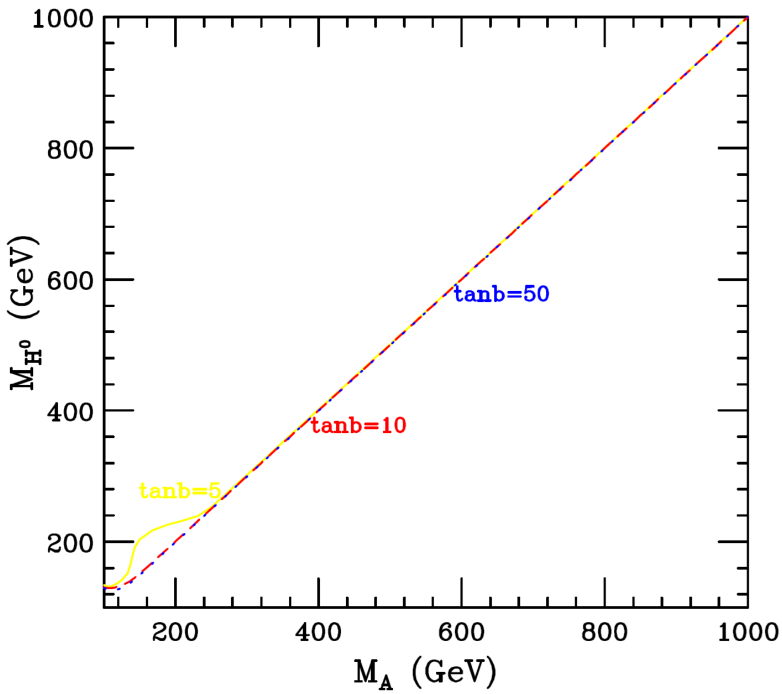

Figure 1.11: Mass of heavy Higgs bosons at one loop correction, different colors correspond to different *tan* β values.

References

[1] A. Martin, R. T. W.J.Stirling, and G. Watt, Eur. Phys J. **C 63**, 189 (2009).

[2] G. Passarino and M. Veltman, Nucl. Phys **160**, 150 (1979).

[3] J. Kuipers, T. Ueda, J. Vermaseren, and J.Vollinga, comput. Phys. Commun. **184**, 1453 (2013).

[4] D. de Florian and J. Mazzitelli, Phys. Rev. lett. **111**, (2013).

[5] J. Baglio *et al.*, arXiv:1212.5581v2[hep-ph] **2**, (2013).

[6] V. D. Barger, , and R. J. Philips, *Collider Physics Updated Edition* (Westview Press, ADDRESS, 1996).

[7] S. Heinemeyer, W. Hollik, and G. Weiglein, arXiv:hep-ph/981232001 **1**, (1998).